JOURNAL OF PHYSICAL ORGANIC CHEMISTRY
J. Phys. Org. Chem. 2002; **15:** 330–342

Conformational dependence of substituent effects in the solvolyses of the 1,1-diphenyl-2,2,2-trifluoroethyl system

Mizue Fujio,[1]* Hyun-Joong Kim,[1] Md. Khabir Uddin,[1] Soo-Dong Yoh,[2] Zvi Rappoport[1]† and Yuho Tsuno[1]

[1]Institute for Fundamental Research of Organic Chemistry, Kyushu University, Hakozaki, Higashi-ku, Fukuoka 812-8581, Japan
[2]Department of Chemistry Education, Teachers College, Kyungpook National University, Taegu 702-701, Korea

Received 12 January 2002; revised 1 February 2002; accepted 6 February 2002

ABSTRACT: The substituent effects on the solvolysis of 1-X-phenyl-1-Y-phenyl-2,2,2-trifluoroethyl tosylates were analyzed on the basis of the Yukawa–Tsuno equation. For the solvolysis of the symmetrically disubstituted X = Y subseries, an excellent linear correlation was obtained. However, in the solvolyses of series of varying X with a fixed-Y subset, the substituent effects were found to give significantly concave Y–T correlations. The ρ value for the Y–T correlations changes significantly with the fixed Y substituent. There is a qualitative trend of a linear decrease in the ρ value as the fixed-Y substituent of the respective subset becomes more electron donating. The non-linearity of substituent effects was attributed to a substituent-induced conformational change of the transition state, which could be simulated by calculation of the preferred conformation of the intermediate carbocation. A molecular orbital optimization method was applied to determine the preferred conformations of the α,α-diarylcarbenium ions derived from the title systems. The symmetrical carbenium ions X = Y have a preferred propeller shape conformation with twist angles differing by 14° (***E** conformation*), whereas in the unsymmetrical systems X ≠ Y the two aryl rings are much more (>30°) differently twisted in the preferred conformation (***PT** conformation*). The linear correlation found for the symmetrical subseries is essentially an outcome of the ***E** conformation* of the transition state. In unsymmetrical cases, the substituent effect correlation in any Y subset should reflect the conformational arrangements, $\boldsymbol{E}_X$, $\boldsymbol{P}_X$ and $\boldsymbol{T}_X$ of the variable X-aryl group, depending on relative $\bar{\sigma}$ values of X and Y. The substituent effects in the Y-subsets were successfully treated by three different Y-independent correlations for the preferred conformational arrangements: ***E*** correlation for substituents when $(\bar{\sigma}_X - \bar{\sigma}_Y) \cong 0$, $\boldsymbol{P}_X$ correlation when $(\bar{\sigma}_X - \bar{\sigma}_Y) \ll 0$ and $\boldsymbol{T}_X$ correlation for the $(\bar{\sigma}_X - \bar{\sigma}_Y) \gg 0$ class, respectively. Copyright © 2002 John Wiley & Sons, Ltd.

KEYWORDS: α,α-diaryl-α-trifluoromethylcarbenium ion system; solvolysis; substituent effect; Yukawa–Tsuno equation; reactivity–conformation relationship

INTRODUCTION

In α,α-diarylcarbenium ion systems, the kinetic effects of substituents on different aromatic rings are frequently not simply additive. A substituent on one ring modifies the charge distribution at the transition state so that a substituent in the other ring interacts with a charge different from that which would prevail in the absence of the first substituent.

The solvolysis of 1,1-diaryl-2,2,2-trifluoroethyl tosylates reveals a structure–reactivity relationship or a linear substituent effect behavior in the α,α-diarylcarbenium ion systems,[1–5] on which detailed analyses of the substituent effects were carried out on the basis of the Yukawa–Tsuno (Y–T) equation:[6]

$$\log(k/k_0) = \rho(\sigma^0 + r\Delta\bar{\sigma}_R^+) \qquad (1)$$

where σ^0 is the normal substituent constant and $\Delta\bar{\sigma}_R^+$ is the resonance substituent constant measuring the donor capability of π-electron donating substituents.[6b] The parameter r is a measure of the resonance demand of the given reaction, i.e. the degree of resonance interaction between the aryl group and the reaction site in the transition state.[1–3,6] Thus, the Y–T equation allows us to define the intrinsic $\bar{\sigma}$ scale inherent in the system, and to derive the appropriate ρ_X as a reference which enables us to detect non-linearity and non-additivity of substituent effects.

In this system we studied the dependence of the substituent effects of a variable X upon a series of fixed Y substituents.[1–3] A precise Y–T relationship was found

---

*Correspondence to: M. Fujio, Institute for Fundamental Research of Organic Chemistry, Kyushu University, Hakozaki, Higashi-ku, Fukuoka 812-8581, Japan.
E-mail: fujio@ms.ifoc.kyushu-u.ac.jp
†Present address: Department of Organic Chemistry, The Hebrew University of Jerusalem, Jerusalem 91904, Israel.

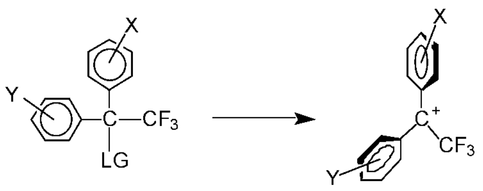

LG = OTs, Br, Cl

1	X = Y	**1C**$^+$
2	X: variable Y = H	**2C**$^+$
3	X: variable Y = *p*-MeO	**3C**$^+$
4	X: variable Y = *p*-Me	**4C**$^+$
5	X: variable Y = *p*-F	**5C**$^+$
6	X: variable Y = *m*-Me	**6C**$^+$
6a	X: variable Y = 3,5-Me$_2$	**6aC**$^+$
7	X: variable Y = *m*-Cl	**7C**$^+$
7a	X: variable Y = *m*-CF$_3$	**7aC**$^+$
7b	X: variable Y = 3,5-Cl$_2$	**7bC**$^+$

previously to hold for the symmetrically disubstituted (X = Y) subseries **1** for a wide range of substituents from (p-MeO)$_2$ to (m-Cl)$_2$ covering a reactivity change of 12 log units, with $2\rho_{sym} = -8.65 \pm 0.16$ and $r_{sym} = 1.17 \pm 0.04$. This simple additivity relationship (X = Y) is

$$\log(k/k_0)_{2X} = 2\rho_{sym}\bar{\sigma}_X = 2\rho_{sym}[\sigma^0_X + r_{sym}(\Delta\bar{\sigma}^+_R)_X] \quad (2)$$

However, a similar simple additivity relationship, against $\bar{\sigma}_X + \bar{\sigma}_Y$, does not hold for the general case with X ≠ Y, and a widely spread pattern is observed instead.

For any fixed-Y subset, the Y–T equation failed to correlate the whole range of substituents with a single slope, at the ordinary precision level of acceptable conformity of Eqn. (1). However, the corresponding Y–T correlation apparently embraced a set of partial Y–T correlations each with different ρ and r values for three different classes of substituents: (a) strong electron-donating groups, (b) weak electron-donating groups including *m*-alkyl and H, and (c) strong electron-withdrawing groups.

The break of the linear correlation indicates that different substituent interaction mechanisms are operating for the different ranges of X substituents within a single subset of a fixed Y. Compared with the reactivity range covered by the linear correlation (2) for the symmetrical subseries, the reactivity change in any fixed Y-subset is in a relatively narrow range. It is therefore unlikely that the non-linearity is due to a change in the reaction mechanism. Most likely, it is closely related to a substituent-induced change in the conformation of the transition state.[1–3,7]

The ArCAr′ moiety in α,α-diarylcarbenium ions adopt a propeller-shaped conformation in order to minimize steric repulsions.[1–3,7] According to the calculation discussed below, in symmetrically disubstituted (X = Y) carbocations **1C**$^+$, both aryl rings are twisted to relatively

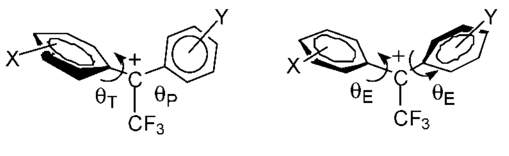

***PT*-conformation** ***E*-conformation**

Scheme 1. Coplanarity change in 1,1-diaryl-2,2,2-trifluoroethyl cation. ***E** conformation*: equivalent propeller conformation ($23 < \theta_E > 38°$); ***PT** conformation*: single aryl twisted conformation ($\theta_P = 9$–$15°$, $\theta_T > 45°$)

slightly different extents with respect to a reference plane including the two *ipso* carbons and the carbenium ion center. This is denoted here as the ***E** conformation* (Scheme 1).[1–3] For unsymmetrical (X ≠ Y) cases, a different conformation is obtained. In order to achieve maximum stabilization through aryl-C$^+$ resonance, the ring carrying the stronger electron donating substituent becomes nearly coplanar with the reference plane ($\theta_P < \sim 10°$) while the less electron-donating ring is appreciably twisted ($\theta_T > \sim 45°$). This conformation is denoted here the ***PT** conformation* (Scheme 1). The conformation where the variable substituents X are located at the coplanar aryl while the fixed substituent Y is located on the twisted ring is denoted here the $\boldsymbol{P}_X$ or $\boldsymbol{P}_X(\boldsymbol{T}_Y)$ *conformation*. The reverse arrangement is denoted the $\boldsymbol{T}_X$ or $\boldsymbol{T}_X(\boldsymbol{P}_Y)$ *conformation*.

The substituent effects on the solvolysis of these systems should reflect the variable geometries of the transition state which can be assumed to resemble the intermediate carbenium ions. The twist angles of the two aryl rings from the reference plane can be related to the relative resonance capabilities of the X- and Y-substituted rings. On the basis of this assumption we have interpreted successfully the non-linear correlations of the substituent effects in these Y subsets in terms of the geometry of the intermediate cations.

In order to extend the scope of this approach, we have examined in detail the substituent effects in fixed Y-subsets comprising both the ***E*** and ***PT*** conformation, which should exhibit all three ***E***, $\boldsymbol{P}_X$ and $\boldsymbol{T}_X$ substituent-dependent reactivities. The substituent effects in the weakly or moderately electron-donating Y-subsets, **5, 6, 6a** and **7a**, in addition to several subsets previously reported, were analyzed by using the Y–T equation. The resulting substituent effect correlations are discussed with respect to the varying coplanarity of the substituted rings in the carbenium ions having the ***E*** and ***PT*** conformations.

RESULTS

Solvolysis data

Most of the solvolyses rate data included in the present study are taken from our previous papers,[1–5] and only

Table 1. Solvolysis rates of 1,1-diaryl-2,2,2-trifluoroethyl bromides, chlorides and tosylates in 80% aqueous ethanol

Substituents		Rate constants[a] 10^5k_t (s^{-1}) at 25 °C or 10^5k_t (s^{-1}) [temperature (°C)]		
X$_1$	X$_2$	k_{Br}[b]	k_{Cl}	k_{OTs}
p-MeO	*p*-OCH$_2$CH$_2$-*m*	*(2.61×10^{5})*	3050[e]	
	p-MeO	*(4.79×10^{4})*	647	
	p-MeS	*(1.284×10^{4})*	173.7	
	p-PhO	*(4440)*	63.3[e]	
	p-MeO-*m*-Cl	*(2690)*	39.3, 39.3[f]	
	p-MeS-*m*-Cl	*(1068)*	16.33	
	3,4-Me$_2$	2210	32.3	
	p-Me	1582	23.5[f]	
	3,5-Me$_2$	741	12.01	
	m-Me	*(611)*	9.60[f]	
	p-F	504	9.82	
	H	467	7.50, 7.64[f]	
	p-Cl	*(279)*	4.56	
	m-Cl	92.5	1.515	
	m-CF$_3$	52.7	0.890[f]	
	p-CF$_3$	*(68.0)*	1.19[f]	
	3,5-Cl$_2$	24.7	0.404	
p-Me	*p*-OCH$_2$CH$_2$-*m*	*(2.68×10^{4})*	349[e]	
	p-MeS	*(307)*	4.99, 49.3 [45]	
	p-PhO	23.0[e]	0.425[e]	
	p-MeO-*m*-Cl	*(17.57)*	0.239	
	p-MeS-*m*-Cl	*(3.94)*	0.0792	
	p-Me	0.388		
	p-*t*-Bu	0.274[c], 3.67 [45], 102.7 [75]		
	3,5-Me$_2$	0.0852[c], 1.229 [45], 37.9 [75]		
	p-F	0.038[d], 0.542 [45]		
	m-Me	0.0428		
	H	0.01896		
	m-Cl			623
	m-CF$_3$			229
3,5-Me$_2$	*p*-MeO-*m*-Cl	5.37		
	p-MeS-*m*-Cl	1.786	(0.0644)[g]	
	H			999
	m-Cl			30.1
	m-CF$_3$			8.83
p-F	*p*-PhO	*(6.61)*	0.1297[c]	
	p-MeO-*m*-Cl	3.127		
	p-MeS-*m*-Cl	1.047, 13.62 [45], 243.4 [75]		
	m-Me			1087
	H			608
	m-CF$_3$			7.20
m-Me	*p*-OCH$_2$CH$_2$-*m*	*(1.489×10^{4})*	200[e]	
	p-PhO	6.88[e]	0.140[e]	
	p-MeO-*m*-Cl	4.07		
	m-CF$_3$			3.31
H	*p*-OCH$_2$CH$_2$-*m*		183[e]	
m-CF$_3$	*p*-MeO-*m*-Cl	0.293, 3.54 (45), 10.73(55), 86.6 [75]		
	3,4-Me$_2$			561

[a] Rate constants experimentally determined in this study are given in regular letters. Rate constants at other temperatures are given together with the measurement temperature in parentheses.

[b] The data in italics are estimated from the observed rate constants of the corresponding chlorides k_{Cl} based on the linear logarithmic rates correlation between k_{Cl} and k_{Br}, see text.

[c] Calculated from data at other temperatures by the Arrhenius equation.

[d] Estimated from the rate constant at 45 °C based on a constant proportionality to the rate constant of 3,5-Me$_2$ derivative.

[e] Taken from rate data reported in Ref. 5.

[f] Taken from rate data reported in Ref. 4.

[g] Excluded from the derivation of the k_{Cl} vs k_{Br} correlation.

new data are given in Table 1. The solvolysis rates of the title substrates with suitable leaving groups (L_G) were measured conductimetrically in 80 vol.% aqueous ethanol (80E) at initial substrate concentrations of ca 10^{-4} mol dm^{-3}. Owing to the remarkable substituent-induced reactivity change of >12 log units, the rate constants k_{LG} of the whole series could not be measured by using a single leaving group. When the solvolysis rates of the tosylates were too fast to follow, the rate constants were determined by solvolyzing the corresponding chlorides or bromides, whereas the rate constants of slow solvolyzing substrates were obtained by solvolysis of the tosylates. The k_{Cl} values were converted into k_{OTs} values by (a) using the linear logarithmic rate correlation between chlorides and bromides, $\log k_{Br} = 1.048 \log k_{Cl} + 1.996$, where k_{Br} and k_{Cl} are the rate constants for solvolyses of the bromide and chloride of the same substrates at 25 °C in 80% aqueous ethanol, and (b) converting the obtained k_{Br} values to the value for the corresponding tosylates k_{OTs} by using a tosylate/bromide rate ratio of 4.24×10^5.[1–3] Estimated k_{OTs} values for a series of fixed-Y subsets, **1**–**7**, at 25 °C are summarized in Table 2.

Analysis of substituent effects

Non-linearity. Correlation analyses of the substituent effects were based on the Y–T equation [Eqn. (1)] for both the symmetrical (Y = X) subseries **1** and the fixed-Y subsets, **2**–**7**, by the ordinary least-squares procedure. Table 3 summarizes the results.

The non-linear behavior of the fixed-Y subsets was analyzed by the More O'Ferrall treatment[8] based on the Taylor expansion approximation (see below), which is used for correlation analysis in the form

$$\log(k_X/k_H)_Y = \rho_0 \bar{\sigma}_X + (2m)_Y(\bar{\sigma}_X)^2 \tag{3}$$

where $\bar{\sigma}_X$ is the Y–T $\bar{\sigma}_X$ parameter scale with $r = 1.17$, ρ_0 is the tangential ρ value at X = H and the coefficient $(2m)_Y$ is a measure of the non-linearity or the deviation from the simple linear free energy relationship. The results are summarized in Table 4.

Non-additivity. The simple additivity relationship Eqn. (2) for the symmetrically disubstituted series **1** was applied for all the substrates with X ≠ Y in the form

$$\begin{aligned}\log(k_{XY}/k_{HH}) &= \rho_{sym}(\bar{\sigma}_X + \bar{\sigma}_Y)\\ &= \rho_{sym}\{(\sigma^0_X + \sigma^0_Y) + r_{sym}[(\Delta\bar{\sigma}^+_R)_X\\ &\quad + (\Delta\bar{\sigma}^+_R)_Y]\}\end{aligned} \tag{4}$$

When $\log(k_{XY}/k_{HH})$ values are plotted against $\bar{\sigma}_X + \bar{\sigma}_Y$ with $r = 1.17$ (Fig. 1), the additivity correlation Eqn. (4) does not hold and a widely spread pattern is observed.

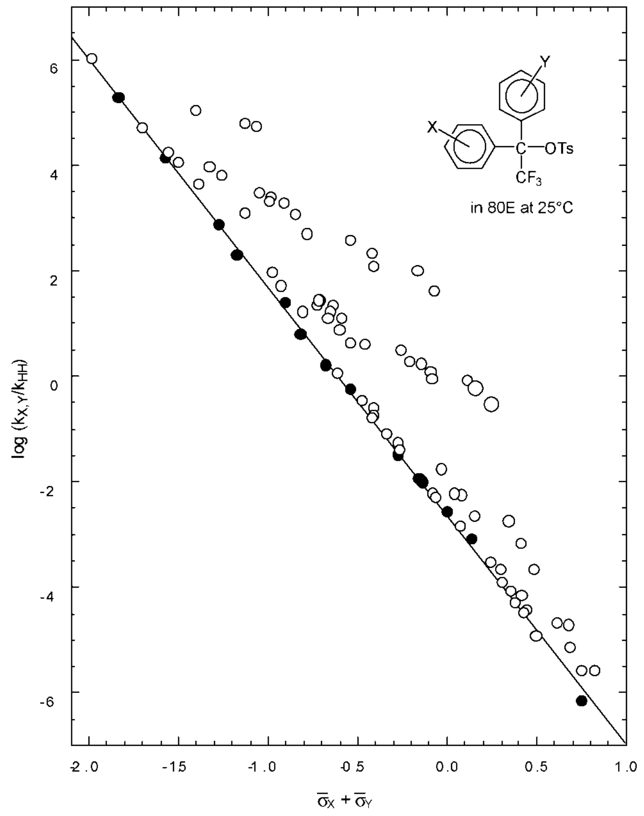

Figure 1. Additivity relationship against the sum of $\bar{\sigma}$ ($r = 1.17$) for substituent effects on the solvolysis of 1,1-diaryl-2,2,2-trifluoroethyl tosylates in 80% aqueous ethanol at 25 °C. Closed circles are for the symmetrical X = Y subseries **1**

However, it applies with a good precision (SD = ±0.13 and $R = 0.9991$) for the closely limited substrates ($n = 36$) where X and Y are similarly conjugative substituents, i.e. only when $(\bar{\sigma}_X - \bar{\sigma}_Y) \rightarrow 0$. There is a significant deviation from additivity in Fig. 1 when $\bar{\sigma}_X$ differs significantly from $\bar{\sigma}_Y$ of the fixed substituent Y.

Conformation of carbenium ions

The structures of the intermediate carbenium ions in our solvolysis reactions were conventionally used as models for the structures of the solvolysis transition states. The geometries of the carbenium ions were obtained by *ab initio* MO calculations.[9] The results of geometry optimizations were partly reported in previous papers,[2,3] and the data derived from the calculation will be completely reported and discussed in a forthcoming paper.

The cations investigated in this study, particularly the parent carbocation $\mathbf{1C}^+$ (X = H), are known to have propeller-shaped conformations. The two phenyls of $\mathbf{1C}^+$ (X = H) in the RHF/6–31G* optimized structure are each rotated by 25.3° and 38.4° from coplanarity with the

Table 2. Solvolysis rate constants[a,b] of 1,1-diaryl-2,2,2-trifluoroethyl tosylates in 80% a queous ethanol at 25 °C

	$k_{OTs}(s^{-1})$ at 25 °C							
Substituent X	*p*-MeO	*p*-Me	*p*-F	3,5-Me_2	*m*-Me	H	*m*-Cl	*m*-CF_3
p-OCH_2CH_2-*m*	11.1×10^5	1.14×10			63200	57500		
p-MeO	2.03×10^5	6710	2140	3151	2590	1980	392	224
p-MeS	54500	1302				523	127.7	
p-PhO	18840	97.6	28.0		29.2	22.4	3.33	1.818
p-MeO-*m*-Cl	11410	53.3	13.28	22.8	17.27	12.92	2.04	1.243
p-MeS-*m*-Cl	4530	16.72	4.44	7.58		4.23	0.883	
3,4-Me_2	9630					0.258	0.01803	0.00561
p-Me	6710	1.646	0.16	0.362	0.1816	0.0805	0.00623	0.00229
3,5-Me_2	3150	0.362		0.0337		0.00999	0.000301	0.0000883
p-F	2140	0.16	0.01194		0.01087	0.00608	0.000223	0.0000720
m-Me	2590	0.1818	0.01087		0.00937	0.00517	0.0001273	0.0000331
H	1980	0.0805	0.00608	0.00999	0.00517	0.00268	0.0000528	0.00001265
p-Cl	1183	0.0548				0.001448	0.0000384	
m-Cl	392	0.00623	0.000223	0.000301	0.0001273	0.0000528	0.000000717	
m-CF_3	224	0.00229	0.0000720	0.0000883	0.0000331	0.00001265		
3,5-Cl_2	104.8	0.000719	0.00001938	0.0000218	0.00000759	0.00000274		

[a] The rate data are mostly taken from those for all the substrates involved in Table 1, in which the k_{Br} of the bromides are converted to k_{OTs} of the corresponding tosylates by using a rate ratio $k_{OTs}/k_{Br} = 4.243 \times 10^5$.

[b] The rate constants for other substrates are taken from Refs 1–3.

Table 3. Correlation analyses of substituent effect[a] for specified range of substituents

No.	Substrates Subset (Y)[b]	Range of substituents X	Yukawa–Tsuno correlation n[c]	ρ	r	R	SD
1	**1** (X = Y)	Whole range	14	-4.325 ± 0.08	1.173 ± 0.04	0.9994	0.12
2	(X ≅ Y)	Whole range (restricted pais)[d]	36	-4.33 ± 0.07	1.17 ± 0.03	0.9991	0.13
3	**2** (H)	Whole range	19	-4.50 ± 0.30	1.66 ± 0.17	0.994	0.35
4		s-ED (*p*-Coum[g]–*p*-MeS-*m*-Cl)[e]	6	-6.53 ± 0.34	(1.79 ± 0.30)[f]		0.16
5		EW (*m*-CF_3, 3,5-Cl_2)	2	-2.0			
6	**3** (*p*-MeO)	Whole range	17	-2.10 ± 0.24	1.03 ± 0.22	0.972	0.26
7		s-ED (*p*-Coum[g]–*p*-MeO-*m*-Cl)[e]	5	-4.06 ± 0.25	(1.05 ± 0.23)[f]		0.07
8		w-ED-EW (*p*-Me–3,5-Cl)	7	-1.87 ± 0.05	0.88 ± 0.04	0.9991	0.02
9	**4** (*p*-Me)	Whole range	16	-3.71 ± 0.39	1.56 ± 0.26	0.987	0.41
10		s-ED (*p*-Coum[g]–*p*-MeO-*m*-Cl)[e]	6	-6.61 ± 0.32	(1.39 ± 0.20)[f]		0.09
11		EW (*m*-CF_3, 3,5-Cl_2)	2	-2.2			
12	**5** (*p*-F)	Whole range	11	-3.92 ± 0.41	1.63 ± 0.26	0.992	0.35
13		s-ED (*p*-MeO–*p*-MeS-*m*-Cl)[e]	4	-6.19 ± 0.43	(1.48 ± 0.36)[f]		0.14
14	**6** (*m*-Me)	Whole range	11	-4.27 ± 0.53	1.72 ± 0.32	0.993	0.43
15		s-ED (*p*-Coum[g]–*p*-MeO-*m*-Cl)[e]	4	-6.74 ± 0.37	(1.45 ± 0.23)[f]		0.10
16	**6a** (3,5-Me_2)	Whole range	9	-4.04 ± 0.35	1.59 ± 0.22	0.995	0.31
17		s-ED (*p*-MeO–*p*-MeS-*m*-Cl)[e]	4	-6.19 ± 0.54	(2.57)[f]		0.19
18	**7** (*m*-Cl)	Whole range	13	-5.57 ± 0.32	1.59 ± 0.13	0.9974	0.22
19		s-ED (*p*-MeO–*p*-MeS-*m*-Cl)[e]	5	-6.50 ± 0.50	(1.84 ± 0.41)[f]		0.18
20		ED (*p*-MeO–*p*-Me)	7	-6.19 ± 0.52	1.57 ± 0.20	0.996	0.19
21	**7a** (*m*-CF_3)	Whole range	9	-6.26 ± 0.40	1.51 ± 0.13	0.9987	0.15
22		s-ED (*p*-MeO–*p*-MeO-*m*-Cl)[e]	4	-6.73 ± 0.34	(1.51 ± 0.07)[f]		0.06

[a] The data are taken in part from Refs 1–3.
[b] Subset with a fixed Y substituent; for abbreviations see text.
[c] Number of substituents involved.
[d] Symmetrical series **1** and unsymmetrical derivatives having pairs of substituents in the same resonance class; see text.
[e] Strong electron-donating iso-resonance class substituents; see text.
[f] The *r* value should be statistically indefinite.
[g] Dihydrobenzofuranyl.

carbocation center; the angles are much closer at higher level (MP2/6–31G*). The difference in the rotation angles of two rings in the preferred conformation does not appear to be energetically very important. Indeed, the bond orders of two benzylic bonds are identical. Moreover, it is likely that a degenerate rapid exchange of the two rings can take place. The slight difference in the twist angle should be due to geometric non-equivalence of the interaction of two aryl groups with the $\alpha{-}CF_3$ group. Essentially the same optimized conformation is obtained for symmetrically disubstituted carbenium ions $\mathbf{1C}^+$ from X = *p*-MeO to X = 3,5-Cl_2.

The preferred optimized conformations of the monosubstituted carbenium ion $\mathbf{2C}^+$ (X = *p*-MeO) is the ***PT***

Table 4. Correlation analyses of substituent effecs[a]

Substrate No.	Subset (Y)[b]	More O'Ferrall correlation [Eqn. (3)] n[c]	ρ_0	$2m$	R	SD
1	**1** (Y = X)	14	-4.325 ± 0.08	0.00	(1.000)	
2	**3** (Y = *p*-MeO)	17	-1.73 ± 0.11	0.66 ± 0.18	0.984	0.20
3	**4** (Y = *p*-Me)	16	-3.91 ± 0.07	1.61 ± 0.11	0.9987	0.12
4	**6a** (Y = 3,5-Me_2)	9	-4.74 ± 0.14	1.49 ± 0.29	0.9976	0.22
5	**6** (Y = *m*-Me)	11	-4.90 ± 0.08	1.65 ± 0.13	0.9994	0.13
6	**5** (Y = *p*-F)	11	-4.64 ± 0.22	1.64 ± 0.22	0.9982	0.17
7	**2** (Y = H)	18	-5.14 ± 0.13	1.70 ± 0.25	0.997	0.24
8	**7** (Y = *m*-Cl	13	-6.23 ± 0.58	1.70 ± 0.81	0.991	0.41
9	**7a** (Y = *m*-CF_3)	9	-7.03 ± 1.13	1.20 ± 1.37	0.994	0.32
10	**7b** (Y = 3,5-Cl_2)	11	-6.61 ± 1.05	1.98 ± 1.24	0.992	0.35

[a] The data are taken from Table 2 and in part from Refs 1–3.
[b] For abbreviations, see text.
[c] Number of substitutes involved.

Table 5. Dihedral angles (°)[a] in the RHF/6–31G* optimized structures of α-(trifluoromethyl)diarylmethyl cations[2,3]

C^+(Y)[b]	**3C$^+$** (*p*-MeO)		**4C$^+$** (*p*-Me)		**2C$^+$** (H)		**7C$^+$** (*m*-Cl)		**7bC$^+$** (3,5-Cl_2)	
X	θ_Y[c]	θ_X[c]	θ_Y[c]	θ_X[c]	θ_Y[c]	θ_X[c]	θ_Y[c]	θ_X[c]	θ_Y[c]	θ_X[c]
p-MeO	22.8	36.9[d]	46.8	15.3	*51.2*	*12.4*[e]	*53.9*	*10.7*[e]	*57.3*	*9.2*[e]
p-Me	15.3	46.8	24.8	37.7[d]	43.5	19.6	46.8	16.6	*53.3*	*12.5*[e]
H	*12.4*	*51.2*[e]	19.6	43.5	25.3	38.4[d]	42.0	21.5	45.7	18.7
m-Cl	*10.7*	*53.9*[e]	16.6	46.8	21.5	42.0	25.0	38.4[d]	42.6	21.5
3,5-Cl_2	*9.2*	*57.3*[e]	*12.5*	*53.3*[e]	18.7	45.7	21.5	42.6	25.6	39.0[d]

[a] Dihedral angles θ_Y, θ_X of the aryl rings from the reference plane of the carbocation.

[b] For abbreviations, see text.

[c] θ_Y = the twist angle of the fixed Y–Ar ring, θ_X = the angles of the variable X–Ar rings.

[d] Angles (underlined) of the limiting structure, *lim **E***-conformation; θ_Y and θ_X are exchangeable.

[e] Angles given in italic are referred to the limiting structure, *lim **PT***-conformation; see text.

conformation with much larger difference in the twist angle of the two aryl rings, due to the fact that one ring is extensively twisted and the other nearly coplanar.

The pairs of the dihedral angles, θ_X and θ_Y, of the optimized conformations are tabulated as in Table 5. For the subseries **1C$^+$** where X = Y or ($\overline{\sigma}_X - \overline{\sigma}_Y$) = O, then is the same preferred propeller ***E*** conformation. Ions where X ≠ Y or ($\overline{\sigma}_X - \overline{\sigma}_Y$) ≠O display a ***PT*** *conformation*. The carbenium ion exists in ***P***$_X$ or ***P***$_X$(***T***$_Y$) *conformation* ($\theta_X = 9 - 15°$), when X are more electron donating than Y in the fixed-Y subset, and the cation takes the ***T***$_X$ or ***T***$_X$(***P***$_Y$) conformation ($\theta_X > 45°$ with $\theta_Y = 9 - 15°$), when X are less electron donating than the fixed-Y substituent.

Thus in the columns for the subsets Y = H and *p*-Me in Table 5, the cations with X = *p*-MeO must have a ***PT*** *conformation*, except that an ***E*** *conformation* is assigned for X = *p*-Me and H. When X is electron withdrawing, the molecule adopts the ***PT*** *conformation*. For cations **3C$^+$**(Y = *p*-MeO), expected when X = *p*-MeO which has the ***E*** *conformation*, all the cations with less electron-donating X substituents than *p*-Me have an optimized ***PT*** *conformation*. The *p*-MeO members of the respective Y subsets at the right-hand side of the first row are the same substrates as the corresponding X members in the first column, Y = *p*-MeO, and have identical optimized conformation to each other.

At both limits, where $|\overline{\sigma}_X - \overline{\sigma}_Y|$ becomes significantly large, the conformation approaches that of a one coplanar aryl and one aryl-twisted conformation with the *limiting dihedral angles* of $\theta_P = 9 - 12°$ and $\theta_T > \sim 50°$, respectively, as indicated in italics in Table 5. This *limiting* conformation is denoted as the *lim **PT** conformation*.

DISCUSSION

From the survey of the correlation results in Table 3, the apparent ρ values for the overall Y–T correlations change significantly with the fixed-Y substituent, and qualitatively ρ decreases linearly as the fixed substituent Y becomes more electron donating. This dependence appears to be in accord with the expectation from the reactivity–selectivity relationship,[8,10,11] which is intimately related to the Hammond–Leffler rate-equilibrium relationship (or the extended Brønsted relationship)[12] concerning the transition state coordinate.

Nevertheless, it is of greater importance that the unsymmetrical subsets where X ≠ Y failed to give a single linear correlation over the whole substituent range. Because of the low precision of the fit in Table 3, it is difficult to decide whether the Y–T equation [Eqn. (1)] fails to correlate the substituent effects in subsets **3** (Y = *p*-MeO) and **4** (Y = *p*-Me). Liu *et al.*[5] pointed out that the Y–T correlation with a high *r* value of 1.8 obtained for a subset with Y = *p*-PhO gave a little improvement over the linearity obtained by using the Brown σ^+, and cast doubt on the real merit of introducing an additional parameter *r*.

Similarly, for subsets **5, 6** and **6a** where *Y* = *p*-F, *m*-Me and 3,5-Me_2, the Y–T equation is insufficiently capable of precisely correlating the effect of the whole X-substituent range as a single linear correlation of acceptable conformity, but it is capable of detecting the break of the linear substituent effect correlation in the α,α-diaryl series.

Whereas the Y–T equation provides excellent correlation (R = 0.999) for subset **7a**, it appears to give more or less significantly non-linear correlations even for **7** (Y = *m*-Cl) and for the monosubstituted subset **2** (Y = H).

The set of strong electron-donating substituents, *p*-OCH_2-CH_2-*m*, *p*-MeO, *p*-MeS and *p*-PhO, in addition to *p*-MeO-*m*-Cl and *p*-MeS-*m*-Cl, have nearly the same $\Delta\overline{\sigma}_R^+$ parameters of -0.70 ± 0.06, contrary to a significant variations of >0.55 $\overline{\sigma}$-units of their σ^0 constants. Consequently, similarly to the set of *m*-substituents, this iso-resonance substituent set provides a convenient method to estimate the real ρ value, denoted ρ_{ED}, for the relevant reactivity range in any subset, while giving an indefinite *r* value for any Y subset. In fact, while a small ρ_{ED} value of −4.2 for the electron-donating range of substituents was obtained for the subset Y = *p*-MeO, constant ρ_{ED} values of -6.46 ± 0.24 were obtained for all the other subsets, ranging from Y = *p*-Me to 3,5-Cl$_2$. Obviously, the Y–T correlations for the whole range of substituents should be non-linear or sharply bilinear in all subsets. It is therefore remarkable that a precise Y–T relationship holds for the whole range of symmetrical substituents (X = Y) subseries **1** where the reactivity changes enormously.

We conclude that the significant non-linearity of substituent effect in any Y subset is irrelevant to the use of the Y–T equation [Eqn. (1)]. The failure in delineating the substituent effects in these Y subsets is not due to a deficiency of the Y–T equation but is caused by an inherent non-linearity of the substituent effects in the α,α-diaryl system.

The simple additivity relationship, Eqn. (4), against $\bar{\sigma}_X + \bar{\sigma}_Y$ instead of $2\bar{\sigma}_X$ gives a widely spread pattern (Fig. 1). All the fixed-Y subsets give significant concave correlations, each of which contacts the correlation line for subseries **1** at the point X = Y. The tangent ρ value at this point of any Y subset should be identical with the ρ_{sym} value for the symmetrical subseries. The same behavior has been observed in other α,α-diarylcarbenium ion reactions, e.g. in solvolyses of benzhydryl chlorides[13,14] and α,α-diarylethyl *p*-nitrobenzoates (M. Fujio *et al.*, Unpublished results), and in the bromination and hydration of α,α-diarylethylenes.[7]

The non-linear correlations have been treated by a More O'Ferrall analysis [Eqn. (3)]. The results in Table 4 lead to the same conclusions as those from the Y–T analysis. The ρ_0 value, i.e. the tangent ρ value at X = H, becomes more negative as Y becomes more electron attracting, and all the correlations are significantly concave with the same degree of curvature, i.e. with essentially the same m_X coefficient, except for Y = *p*-MeO.

A large $(2m)_Y$ coefficient in Eqn. (3) indicates a non-linearity of the Hammett-type relationship, and the concave correlation for the respective Y-subset should relate to the anti-Hammond shift of the transition state coordinate (or a late transition state) for rate-accelerating substrates, if this might be ascribed to the shift of the transition state coordinate.[8] However, this conflicts with the conclusion deduced above from the behavior of the ρ values for the whole substituent set (Table 3).

In these non-linear correlation analyses, we have used the reference $\bar{\sigma}$ values ($r = 1.17$) defined for symmetrical subseries **1**. However, it is important that in the non-linear substituent effect correlations for varying fixed-Y subsets, the *r* value should vary with the fixed-Y substituent. Thus for instance, the reactivities of *p*-MeS-*m*-Cl and 3,4-Me$_2$ are the same in the symmetrical subseries **1**, the apparent $\bar{\sigma}$ values of both substituents being identical at an *r* value of 1.17. In subset **3** (Y = *p*-MeO), *p*-MeS-*m*-Cl is clearly less reactive than 3,4-Me$_2$, with the *r* value for this subset being <1.17. On the other hand, *p*-MeS-*m*-Cl is more reactive than 3,4-Me$_2$ in Y = H and *m*-Cl subsets, with $r > 1.17$. Furthermore, in subsets **7** (Y = *m*-Cl) and **7a** (Y = *m*-CF$_3$), the reactivities of *p*-MeO-*m*-Cl and *p*-MeS-*m*-Cl derivatives are distinctly higher than those of the *p*-alkyls, in line with $r = 1.5$ in the Y–T correlations for these subsets (Table 3).

These complicated substituent–reactivity relationships are incompatible with the widely accepted interpretation of a mechanistic change or a coordinate shift of the transition state. The non-linearity and/or non-additivity in the substituent effects observed in our system seem to arise from a substituent-induced change of the conformation of the transition state.

Conformation–reactivity relationship

In previous papers,[2,3] such complicated non-linearity and non-additivity behaviors were ascribed to a substituent-dependent conformation of the incipient carbenium ions.

The reactivity data matrix of the X and Y substituents in Table 2 can be compared with the MO structural parameters of the carbenium ions in Table 5. The reactivities of substrates with X ≠ Y or at a limit $(\bar{\sigma}_X - \bar{\sigma}_Y) \rightarrow 0$ are referred to as inherent substituent effects of the ***E***-conformation. The reactivities when **X ≠ Y** are referred to as the inherent substituent effects in the ***PT*** conformation, and those at the limits, where $|\bar{\sigma}_X - \bar{\sigma}_Y|$ becomes highly significant, are regarded as inherent in the *lim* ***PT*** conformation. In any fixed-Y subset, the parent conformation of the transition state varies from the ***E***-conformation when X = Y to the ***PT*** conformation when **X ≠ Y** arrive at the *lim* ***PT*** conformation at both limits of the substituent set. A change in the preferred transition state conformation with the increase in $|\bar{\sigma}_X - \bar{\sigma}_Y|$ appears to be the major cause of the non-linearity of substituent effects.

It is reasonable to assume that a linear Y–T relationship [Eqn. (1)] generally holds for systems where the transition state conformation remains constant. This is the only requirement for applying the linear regression analysis to the present system.

The *lim* $\boldsymbol{P}_X$ correlation (5) should be given for the $\boldsymbol{P}_X(\boldsymbol{T}_Y)$ arrangement of a given fixed-Y subset:

$$[\log(k_X/k_H)_Y]_P = \rho_P(\bar{\sigma}_X)_P = \rho_P(\sigma^0 + r_P\Delta\bar{\sigma}_R^+) \quad (5),$$

and the $\boldsymbol{T}_X$ correlation for the $\boldsymbol{T}_X(\boldsymbol{P}_Y)$ arrangement of fixed-Y subset by Eqn. (6):

$$[\log(k_X/k_H)_Y]_T = \rho_T(\bar{\sigma}_X)_T = \rho_T(\sigma^0 + r_T\Delta\bar{\sigma}_R^+) \quad (6).$$

The two correlation lines should intersect for the symmetrical X = Y member at $(\bar{\sigma}_Y)_{\boldsymbol{P}} + (\bar{\sigma}_Y)_{\boldsymbol{T}}$, and the $[\log\,(k_Y)_Y]_{\boldsymbol{PT}}$ value at the intersection point should refer to the reactivity of the X = Y member of *lim* ***PT*** conformation. The $\boldsymbol{P}_X(\boldsymbol{T}_Y)$ and $\boldsymbol{T}_X(\boldsymbol{P}_Y)$ correlations of a

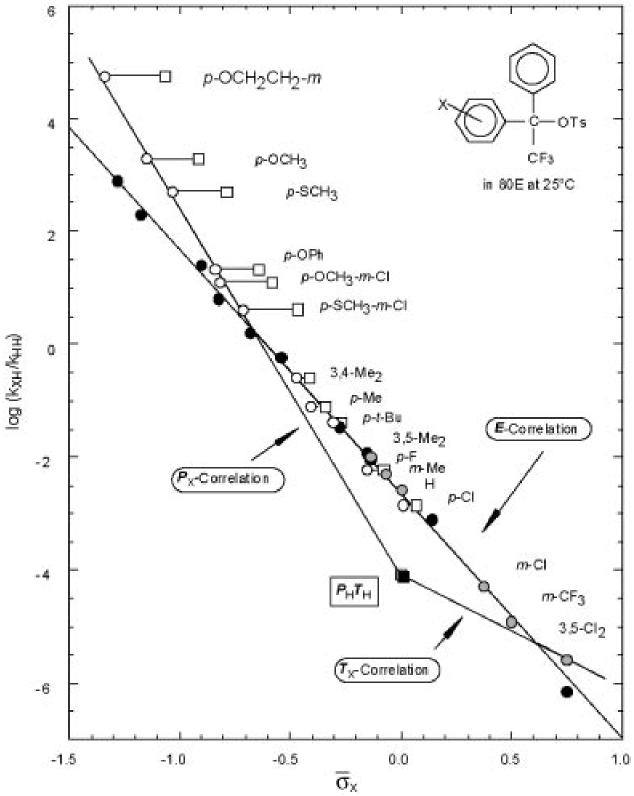

Figure 2. The Y–T plot for the solvolysis of 1-phenyl-1-(substituted phenyl)-2,2,2-trifluoroethyl tosylates (**2**). Open squares for the ***E***-conformer correlation against $\bar{\sigma}_E$ with $r = 1.17$, open circles for the $\boldsymbol{P}_X$-conformer correlation against $\bar{\sigma}_P$ with $r = 1.505$, gray circles for *m*-substituents against σ^0 and black circles for symmetrically disubstituted substrates defining the ***E***-conformer correlation

subset (Y) with *lim* ***PT*** conformation should be defined by the tangent correlation lines at the strong electron-donating and -withdrawing ends of the non-linear (concave) plot of the whole-substituents correlation for a given Y subset. Thus, by extrapolating the $\boldsymbol{P}_X(\boldsymbol{T}_Y)$ and $\boldsymbol{T}_X(\boldsymbol{P}_Y)$ correlations, the behavior of the *lim* ***PT*** conformer of the substrates with $\bar{\sigma}_X \cong \bar{\sigma}_Y$, which is otherwise hidden below the line for the preferred ***E*** conformer correlation could be obtained.

This analytical procedure was applied to typical fixed-Y subsets in the present system.

The *lim PT* conformation correlation of the reference subset 2. In the monosubstituted subset **2** (Y = H), all substituents in the range *p*-alkyl–*m*-Cl should obey an ***E***-conformation correlation. Both the $\boldsymbol{P}_X$ and $\boldsymbol{T}_X$ correlations can be described by the tangential correlation lines (against appropriate $\bar{\sigma}$ scales) at the electron-donating and -withdrawing ends of the substituent set. Since the X = 3,5-Cl_2 point in subset **2** (Y = H) lies clearly above the ***E***-conformer line, that may be recognized as belonging to the *lim* $\boldsymbol{T}_X$ arrangement. The *lim* $\boldsymbol{T}_X$ reactivities of X = *m*-CF_3 and *m*-Cl can be estimated by extrapolating the $\boldsymbol{P}_X$ correlations of **7a** and **7** to the origins (X = H). The Y–T plots of the pair of $\boldsymbol{P}_X(\boldsymbol{T}_H)$ and $\boldsymbol{T}_X(\boldsymbol{P}_H)$ correlations of subset **2** with a *lim* ***PT*** conformation are illustrated in Fig. 2. The two ends of the concave correlation in the negative $\bar{\sigma}$ range of the $\boldsymbol{P}_X$ correlation and the positive end of the $\boldsymbol{T}_X$ correlation that lie above the reference ***E*** line could be experimentally detectable. As the crossing point of the two tangent lines, we can define the specific reactivity $[\log (k_H)_{\mathbf{2}}]_{\boldsymbol{PT}} = -4.08$ for the *lim* ***PT*** conformer of the parent compound **2** (X = Y = H), which should be referred to as the general origin ($\bar{\sigma} = 0.00$) in the $\bar{\sigma}$ scale. This $[\log (k_H)_{\mathbf{2}}]_{\boldsymbol{PT}}$ value is 1.50 log-units lower than the experimental $[\log (k_H)_{\mathbf{2}}]_E$ value assigned to the origin of the preferred ***E*** conformer correlation.

The plot of X substituents in the $\boldsymbol{P}_X$ correlation of subset **2** (Y = H) is referred to as the trace of the zero points of the *lim* ***T*** correlations, i.e. the origins $(\bar{\sigma})_{\boldsymbol{T}} = 0$, of the corresponding X-fixed subsets, and the plot of X in the *lim* $\boldsymbol{T}_X$ correlation of **2** is referred to as the trace of the zero points $[(\bar{\sigma})_{\boldsymbol{P}} = 0]$ in the case of the *lim* ***P*** correlations of the X-fixed subsets. The $\boldsymbol{P}_X$ and $\boldsymbol{T}_X$ correlation lines for **2** (Y = H) serve as the reference axes for the $\boldsymbol{P}_X$ and $\boldsymbol{T}_X$ coordinates in the quantitative analysis of substituent effects.

The *lim PT*-conformer correlation of *meta*-substituted subsets. The *lim* ***PT***-conformer analysis was carried out for the subsets with fixed *meta*-substituents Y = *m*-Me and 3,5-Me_2. As the $\boldsymbol{P}_X$ $(\boldsymbol{T}_Y)$, $\boldsymbol{T}_X$ $(\boldsymbol{P}_Y)$ and ***E*** conformers substituent effects in these *meta*-substituent fixed-Y subsets are close to those in the reference subset **2** (Y = H), the *lim* $\boldsymbol{P}_X$ $(\boldsymbol{T}_Y)$ and $\boldsymbol{T}_X$ $(\boldsymbol{P}_Y)$ reactivities can be analyzed in terms of the $\boldsymbol{P}_X$ and $\boldsymbol{T}_X$ coordinates defined above (Table 6). Figure 3 demonstrates the substituent effect correlations for the three conformational arrangements in these subsets against the sum of $\bar{\sigma}_X + \bar{\sigma}_Y$. The $(\bar{\sigma})$ parameters for these *meta*-substituents (Y) are given here by the *r*-independent σ^0 values irrespective of the ***E***, ***P*** and ***T*** arrangements.

Thus, the *lim* $\boldsymbol{P}_X$ correlation of subset **6** or **6a** is defined, based on experimental log $(k_X)_{\mathbf{Y}}$s, for strong electron-donating substituents including the log $(k_H)_{\mathbf{Y}}$ as the origin ($\bar{\sigma}_X = 0$) of the $\boldsymbol{P}_X$ correlation of each Y subset, **6** or **6a**, which corresponds to the point X = *m*-Me or 3,5-Me_2 on the $\boldsymbol{T}_X$ axis. Whereas the $\boldsymbol{P}_X$ correlations ($\rho_{\boldsymbol{P}}$ and $r_{\boldsymbol{P}}$ values) for these weak *m*-Y subsets have to be the same as those of the reference subset **2** (Y = H), the $\boldsymbol{T}_X$ correlation for either **6** or **6a** can be defined based on the experimental log $(k_X)_{\mathbf{Y}}$s for X = *m*-CF_3 and 3,5-Cl_2, including the log $(k_H)_Y$ of the $\boldsymbol{T}_X$-origin of **6** or **6a**, which corresponds to the $(\bar{\sigma}_X)_{\boldsymbol{P}}$ point on the $\boldsymbol{P}_X$ axis for either of these groups.

The *lim* $\boldsymbol{P}_X$ correlation of subset **7** (Y = *m*-Cl) based on electron-donating substituents down to *p*-Me is parallel to the $\boldsymbol{P}_X$ axis with essentially the same $\rho_{\boldsymbol{P}}$ and $r_{\boldsymbol{P}}$,

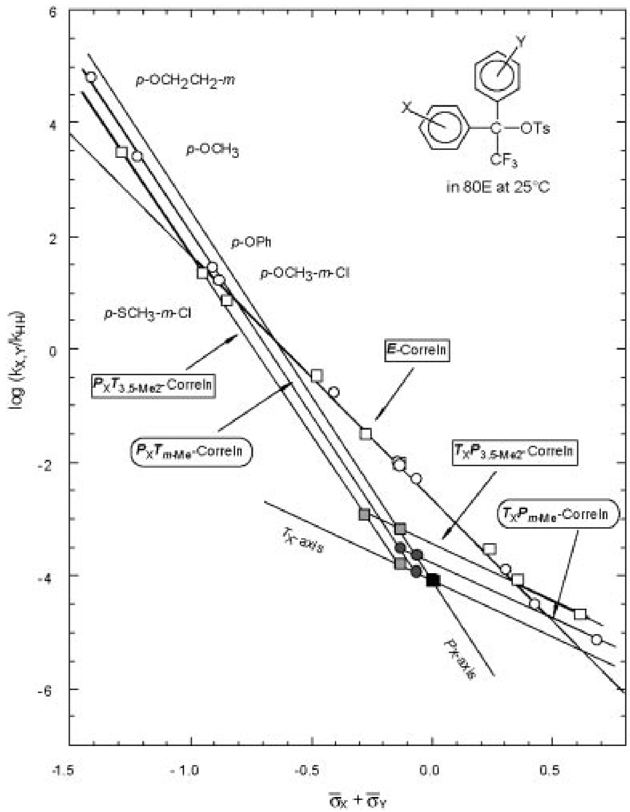

Figure 3. The Y–T plot for the solvolyses of 1-aryl-1-(*m*-methylphenyl)-2,2,2-trifluoroethyl tosylates (**6**) and 1-aryl-1-(3,5-dimethylphenyl)-2,2,2-trifluoroethyl tosylates (**6a**). Open circles are for **6**, open squares for **6a**, and closed symbols for *lim* ***PT***-conformation (see text)

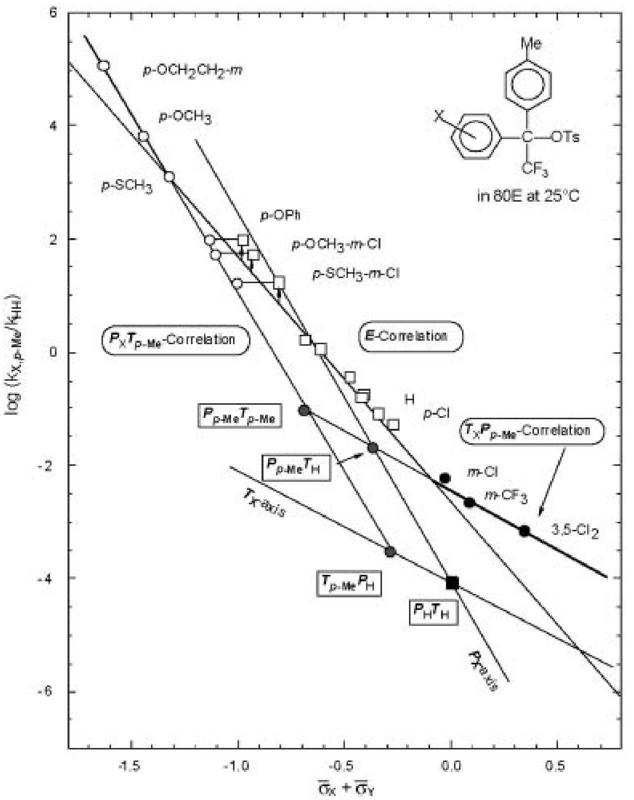

Figure 4. The Y–T plots for the solvolyses of 1-aryl-1-(*p*-methylphenyl)-2,2,2-trifluoroethyl tosylate (**4**). Open circles are for the $\boldsymbol{P}_{\mathrm{X}}$-conformer correlation against $\bar{\sigma}_{\mathrm{P}}$ ($r = 1.505$), open squares are for the ***E***-conformer correlation against $\bar{\sigma}_{\mathrm{E}}$ ($r = 1.17$) and closed circles are for the *lim* $\boldsymbol{T}_{\mathrm{X}}$ correlation against $\bar{\sigma}_{\mathrm{T}}$ ($= \sigma^0$)

intercepting the $\boldsymbol{T}_{\mathrm{X}}$ axis at $(\bar{\sigma}_{\mathrm{X}})_{\boldsymbol{T}}$ for the *m*-Cl substituent (Table 3). This *lim* $\boldsymbol{P}_{\mathrm{X}}$ $(\boldsymbol{T}_{m\text{-Cl}})$ correlation was extrapolated to the origin (at X = H) in order to define the $\boldsymbol{T}_{\mathrm{X}}$ reactivity, $[\log (k_{m\text{-Cl}})_{\mathrm{H}}]_{\boldsymbol{PT}}$, of **2** (X = *m*-Cl), and also to define $[\log (k_{m\text{-Cl}})_{\mathrm{Y}}]_{\boldsymbol{PT}}$ values as $\boldsymbol{T}_{\mathrm{X}}$ reactivities for any Y-subsets.

The *lim PT* conformer correlations of subsets with weak electron-donating substituents Y, 4 and 5. The behavior of subset **5** (Y = *p*-F) is close to those of **6** (Y = *m*-Me) and **6a** (Y = 3,5-Me$_2$), and the *lim* ***PT*** substituent effect has been similarly analyzed in terms of the $\boldsymbol{P}_{\mathrm{X}}$ and $\boldsymbol{T}_{\mathrm{X}}$ coordinates. The $\boldsymbol{T}_{\mathrm{X}}$ correlation line for **5** based on the points for X = *m*-CF$_3$ and 3,5-Cl$_2$ lies on the $\boldsymbol{T}_{\mathrm{X}}$ line for **6a** (Y = 3,5-Me$_2$), being parallel to the $\boldsymbol{T}_{\mathrm{X}}$ axis and intersecting the $\boldsymbol{P}_{\mathrm{X}}$ axis at the point X = *p*-F. Thus $(\bar{\sigma}_{p\text{-F}})_{\boldsymbol{P}}$ of *p*-F in the *lim* ***PT*** correlation should be equal to the $(\bar{\sigma}_{3,5\text{-Me}2})_{\boldsymbol{P}}$ value of −0.14 for 3,5-Me$_2$. The plots for the middle range of substituents *p*-Me to *m*-Cl fall on the ***E*** correlation line. The *lim* $\boldsymbol{P}_{\mathrm{X}}$ correlation essentially coincides with the $\boldsymbol{P}_{\mathrm{X}}$ axis intercepting the $\boldsymbol{T}_{\mathrm{X}}$ axis at $(\bar{\sigma}_{p\text{-F}})_{\boldsymbol{T}} = -0.01$, which implies that the $\boldsymbol{r}_{\boldsymbol{T}}$ value for the reference *lim* $\boldsymbol{T}_{\mathrm{X}}$ correlation for subset **2** (Y = H) should be ca 0.90.

The substituent effects of the subset **4** (Y = *p*-Me) are displayed in Fig. 4 with reference to the $\boldsymbol{P}_{\mathrm{X}}$ and $\boldsymbol{T}_{\mathrm{X}}$ axes (drawn as thin lines). The *lim* $\boldsymbol{T}_{\mathrm{X}}$ correlation ($\rho_{\boldsymbol{T}} = -2.0$) was practically defined by the line passing through the points for X = 3,5-Cl$_2$ and *m*-CF$_3$, and especially the zero point (X = H), which corresponds to the point $(\bar{\sigma}_{p\text{-Me}})_{\boldsymbol{P}}$ on the $\boldsymbol{P}_{\mathrm{X}}$ axis. The *lim* $\boldsymbol{P}_{\mathrm{X}}$ correlation was based on the strong electron-donating substituents including the point $(\bar{\sigma}_{p\text{-Me}})_{\boldsymbol{T}}$ on the $\boldsymbol{T}_{\mathrm{X}}$ axis as the origin $(\bar{\sigma}_{\mathrm{X}})_{\boldsymbol{P}} = 0.0$ (for X = H). The results are given in entries 6 and 7 of Table 6.

The ρ and r values of the $\boldsymbol{P}_{\mathrm{X}}$ correlations in the *lim* ***PT*** conformation system are constant irrespective of the varying Y, and the $\boldsymbol{T}_{\mathrm{X}}$ correlation is also constant for all the Y subsets examined. This implies that any Y subset in the *lim* ***PT*** conformation system should have essentially identical substituent effect correlation; the r and ρ values remain nearly the same in either the $\boldsymbol{P}_{\mathrm{X}}$ or the $\boldsymbol{T}_{\mathrm{X}}$ correlation irrespective of Y, while closer examinations are required for a wider range of Y subsets.

In the case of **3**, Y = *p*-MeO, even though all the strong electron-donating class substituents are correlated entirely with the ***E*** conformer correlation, Eqn. (2), an entire range of X substituents more electron-withdrawing

Table 6. Correlation analyses of substituent effects for specified conformational arrangements of aryl substituent

Substrates		Substituent X		Yukawa-Tsuno correlation				
No.	Set (Y)	Conformation[b]	Substituent range	*n*[c]	ρ	*r*	*R*	SD
1	**1** (X = Y)		Whole range[a]	14	-4.325 ± 0.08	1.173 ± 0.04	0.9994	0.12
2	(X ≅ Y)	$\mathit{lim}.\boldsymbol{E}$[b]	Whole range (restricted pairs)[d]	36	-4.33 ± 0.06	1.17 ± 0.03	0.9991	0.13
3	**2** (H)	$\boldsymbol{P}_X$	(*p*-Coum[h]–*p*-MeS-*m*-Cl), H[e]	7	-6.52 ± 0.24	1.505 ± 0.084	0.9994	0.12
4		$\boldsymbol{T}_X$	(*m*-CF_3-3,5-Cl_2), *m*-Cl[f]	3	-1.978 ± 0.08		0.9984	0.03
5	**3** (*p*-MeO)	$\boldsymbol{T}_X$	(*p*-Me - 3,5-Cl_2)	7	-1.84 ± 0.05	0.90 ± 0.04	0.9985	0.04
6	**4** (*p*-Me)	$\boldsymbol{P}_X$	(*p*-Coum[h]–*p*-MeO-*m*-Cl), H[g]	6	-6.23 ± 0.18	1.54 ± 0.06	0.9999	0.06
7		$\boldsymbol{T}_X$	(*m*-CF_3-3,5-Cl_2), *m*-Cl,[i] H[j]	4	-2.1	(0.90)[l]		
8	**5** (*p*-F)	$\boldsymbol{P}_X$	(*p*-Coum[h]–*p*-MeS-*m*-Cl), H[g]	5	-6.25 ± 0.29	1.54 ± 0.01	0.9996	0.10
9		$\boldsymbol{T}_X$	(*m*-Cl, 3,5-Cl_2), H[j]	3	-2	(0.90)[l]		
10	**6** (*m*-Me)	$\boldsymbol{P}_X$	(*p*-Coum[h]–*p*-MeO-*m*-Cl), *p*-Me[k], H[g]	6	-6.74 ± 0.17	1.44 ± 0.05	0.9999	0.06
11		$\boldsymbol{T}_X$	(*m*-Cl, 3,5-Cl_2), H[j]	3	-2			
12	**6a** (*3,5*-Me_2)	$\boldsymbol{P}_X$	(*p*-MeO–*p*-MeS-*m*-Cl), *p*-Me[k], H[g]	5	-6.13 ± 0.24	1.550 ± 0.09	0.9997	0.09
13		$\boldsymbol{T}_X$	(*m*-CF_3, 3,5-Cl_2) H[j]	3	-2			
14	**7** (*m*-Cl)	$\boldsymbol{P}_X$	(*p*-MeO–*p*-MeS-*m*-Cl), H[g]	6	-6.30 ± 0.53	1.55 ± 0.18	0.9983	0.19
15	**7a** (*m*-CF_3)	$\boldsymbol{P}_X$	(*p*-MeO–H)	9	-6.26 ± 0.40	1.506 ± 0.128	0.9987	0.15
16	**7b** (*3,5*-Cl_2)	$\boldsymbol{P}_X$	(*p*-MeO–H)	11	-6.32 ± 0.23	1.56 ± 0.08	0.9992	0.12

[a] The data are taken in part from Refs 1–3.

[b] The limiting conformation of X-Ar included in the correlation (see text).

[c] Number of substituents involved

[d] Symmetrical series **1** and unsymmetrical derivatives having pairs of substituents in the same resonance class; see text.

[e] General origin, see text.

[f] Log *k* is estimated for X = H from the $\boldsymbol{P}_X$-correlation of **7** (Y = *m*-Cl); entry 14.

[g] The reading $\boldsymbol{T}_X$-axis for the substituent Y of a given subset.

[h] Dihydrobenzofuranyl.

[i] Log *k* is estimated for X = *p*-Me from the $\boldsymbol{P}_X$-correlation of **7** (Y = *m*-Cl); entry 14.

[j] The reading $\boldsymbol{P}_X$-axis for the substituent Y of a given subset.

[k] The reading (log *k*) in the $\boldsymbol{T}_X$-correlation of **4** (entry 7) for the substituent Y of a given subset.

[l] Assumed to be same for all the $\boldsymbol{T}_X$-correlations, cf. entry 5.

than *p*-Me can define unambiguously the $\boldsymbol{T}_X$ correlation of **3**. Extrapolation of this correlation yields a point for X = *p*-MeO, ca 0.6 log-units lower than the ***E***-conformer reactivity. Since the origin, $(\bar{\sigma}_X)_{\boldsymbol{P}} = 0$, in the $\boldsymbol{P}_X$ correlation for **3** should correspond to the point $(\bar{\sigma}_{p-\mathrm{MeO}})_{\boldsymbol{T}}$ for X = *p*-MeO in the $\boldsymbol{T}_X$ axis, the ρ value for the $\boldsymbol{P}_X$ correlation of **3** appears to be close to the values for any other Y subsets, while this correlation is experimentally unobservable.

CONCLUSION

We have proposed a linear regression analysis of the non-linear and non-additive substituent effects in the solvolytic generation of the present α,α-diarylcarbenium ions, in terms of the substituent (Y)-induced change of the preferred conformation in the carbenium ion forming transition state.

A simple additivity relationship, Eqn. (2), holds for the ***E***-conformer substituent effects, whereas an extended form of weighted additivity relationships, Eqns (5) and (6), hold for the *lim* ***PT*** conformer system of fixed-Y subsets. The substituent effects in a given Y subset of the diaryl system have to be described by different $\bar{\sigma}$ scale, $(\bar{\sigma}_X)_{\boldsymbol{P}}$ and $(\bar{\sigma}_X)_{\boldsymbol{T}}$ with different *r*s for the different conformational arrangements of the variable X-aryl. In addition, the use of different ρ values, $\rho_{\boldsymbol{P}}$ and ρ_T, for aryls having non-equivalent conformational arrangements are essential for a proper analysis.

For three conformational arrangements of the X-aryl probes, three selectivity parameters, ρ_E, ρ_P and ρ_T, with different *r* values, were obtained for the respective fixed-Y subsets. We found that these selectivity parameters remain constant for the respective aryl arrangements irrespective of varying Y subsets. This led to an important conclusion that there is no coordinate shift of the transition state with the Y substituents in this system.

EXPERIMENTAL

Materials. The trifluoroacetophenones required for the preparation of the alcohol precursors of the solvolysis substrates were synthesized according to Steward's procedure by the Grignard reaction of substituted bromobenzenes with trifluoroacetic anhydride at −78 °C in a dry ice–acetone bath.[15]

Trifluoroacetophenones were converted into the corresponding 1,1-diaryl-2,2,2-trifluoroethanols by the Grignard reaction with substituted phenylmagnesium bromide at ice-bath temperature. The tertiary alcohols obtained were purified by column chromatography on silica gel.

Table 7. Physical and analytical data for 1,1-diaryl-2,2,2-trifluoroethyl alcohols, bromides and tosylate

Substituent (X, Y)	M.p. (°C)	Carbon (%) Calcd	Carbon (%) Found	Hydrogen (%) Calcd	Hydrogen (%) Found
Alcohols					
m-CF_3, 3,4-Me_2	liq.	58.63	58.34	4.05	4.16
m-CF_3, 3,5-Me_2	liq.	58.63	58.47	4.05	4.03
p-MeO-*m*-Cl, 3,5-Me_2	131–132	59.23	59.01	4.68	4.69
p-MeS, 3,4-Me_2	liq.	50.72	50.94	3.72	3.95
p-MeO, 3,4-Me_2	liq.	65.80	66.00	5.52	5.64
p-MeO, 3,5-Me_2	99.5–100.5	65.80	65.69	5.52	5.53
p-MeO, *p*-Cl	liq.	56.89	56.78	3.82	4.03
p-Me, *p*-F	liq.	63.38	63.15	4.26	4.34
p-Me, *m*-CF_3	liq.	57.49	57.41	3.62	3.69
p-MeS-*m*-Cl, *p*-MeS	liq.	50.72	50.94	3.72	3.95
p-MeS-*m*-Cl, *p*-MeO-*m*-Cl	liq.	48.38	48.40	3.30	3.56
Bromides					
p-MeO, 3,4-Me_2	85.5–86.5	54.71	54.72	4.32	4.37
p-MeO, 3,5-Me_2	97–98	54.71	54.77	4.32	4.40
p-Me, *p*-F	liq.	51.90	51.20	3.19	3.34
Tosylate					
p-Me, *m*-CF_3	44–46	56.56	56.35	3.71	4.06

1,1-Diaryl-2,2,2-trifluoroethyl bromides were prepared from the alcohol and phosphorus tribromide by essentially the same procedure as reported by Liu *et al.*[16] The bromide was purified through column chromatography on alumina. Some of the bromides were not easily purified and were directly utilized for the kinetic measurements.

The tosylates were prepared according to Tidwell's method, by a slow reaction of the alcohols with *p*-toluenesulfonyl chloride in the presence of NaH in cold diethyl ether solution under a nitrogen atmosphere.[17] The tosylate esters obtained were purified by recrystallization from diethyl ether–hexane.

Physical constants and analytical data are listed in Table 7.

Solvents. Commercial 95% ethanol was dehydrated twice by heating under reflux with magnesium ethoxide and distilled. Deionized water was refluxed with $KMnO_4$ and the distillate was redistilled immediately before use. The 80% aqueous ethanol (80E) was prepared by mixing the corresponding volumes of ethanol (80) and water (20) at 25 °C.

Kinetic measurements. Solvolysis rates were measured by a conductimetric method as described previously.[1–3] Conductance measurements were made using $\sim$50 cm^3 of 10^{-4}–10^{-5} mol dm^{-3} solution of the substrates (1–2 mg) in a thermostatted bath controlled within $\pm$0.02 °C. Conductance readings were taken automatically by using a conductivity meter (CM-60S, Toa Electronics) connected to a computer. Solvolyses were followed by taking at least 100 readings at appropriate intervals for 2.5 half-lives; the infinity reading was taken after 10 half-lives. The precision of fit to first-order kinetics was generally satisfactory over 2.5 half-lives ($R > 0.99995$). The experimental errors in individual runs were generally <1.5% and rate constants from repeated runs were reproducible within an accuracy of 3%.

REFERENCES

1. Fujio M, Morimoto H, Kim H-J, Tsuno Y. *Bull. Chem. Soc. Jpn.* 1997; **70**: 1403–1411.
2. Fujio M, Morimoto H, Kim H-J, Tsuno Y. *Bull. Chem. Soc. Jpn.* 1997; **70**: 3081–3090.
3. Fujio M, Kim H-J, Morimoto H, Yoh S-D, Tsuno Y. *J. Phys. Org. Chem.* 1999; **12**: 843–857.
4. Yoh S-D, Kweon JM, Byeon SI, Fujio M, Mishima M, Tsuno Y. *Bull. Korean Chem. Soc.* 1996; **17**: 228–234.
5. Liu K-T, Chang S-M, Chen H-I, Chiu P-F, Wu T-R. *J. Org. Chem.* 1991; **56**: 1315–1317.
6. (a) Yukawa Y, Tsuno Y. *Bull. Chem. Soc. Jpn.* 1959; **32**: 971–981; (b) Yukawa Y, Tsuno Y, Sawada M. *Bull. Chem. Soc. Jpn.* 1966; **39**: 2274–2286; (c) Tsuno Y, Fujio M. *Chem. Soc. Rev.*, 1996; **25**: 129–139; (d) Tsuno Y, Fujio M. *Adv, Phys. Org. Chem.* 1999; **32**: 267–385.
7. Dubois JE, Aaron JJ, Alcais P, Doucet JP, Rothenberg F, Uzan R. *J. Am. Chem. Soc.* 1972; **94**: 6823–6828; Hegarty AF, Lomas JS, Wright WV, Bergmann ED, Dubois JE. *J. Org. Chem.* 1972; **37**: 2222–2228.
8. O'Brien M, More O'Ferrall RA. *J. Chem. Soc., Perkin Trans. 2* 1978; 1045–1053.
9. (a) Nakata K, Fujio M, Saeki Y, Mishima M, Tsuno Y, Nishimoto K. *J. Phys. Org. Chem.* 1996; **9**: 561–572; (b) Nakata K, Fujio M, Saeki Y, Mishima M, Tsuno Y, Nishimoto K. *J. Phys. Org. Chem.* 1996; **9**: 573–582.
10. Johnson CD. *Tetrahedron*, 1980; **36**: 3461–3480; Ruasse MF. *Adv. Phys. Org. Chem.* 1993; **28**: 207–291.
11. Dubois JE, Ruasse MF, Argile A. *J. Am. Chem. Soc.* 1984; **106**: 4840–4845; Dubois JE, Argile A, Ruasse MF. *J. Am. Chem. Soc.* 1984; **106**: 4846–4849.

12. Leffler JE, Grunwald E. *Rates and Equilibria of Organic Reactions.* Wiley: New York, 1963.
13. Nishida S. *J. Org. Chem.* 1967; **32**: 2692–2701.
14. Fox JR, Kohnstam G. *Proc. Chem. Soc.* 1964; 115–116.
15. Stewart R, Teo KC. *Can. J. Chem.* 1980; **58**: 2491–2496; Stewart R, Teo KC, Ng LK. *Can. J. Chem.* 1980; **58**: 2497–2503.
16. Liu K-T, Kuo M-Y, Shu C-F. *J. Am. Chem. Soc.* 1982; **104**: 211–215.
17. Allen AD, Jansen MP, Koshy KM, Mangru NN, Tidwell TT. *J. Am. Chem. Soc.* 1982; **104**: 207–211; Allen AD, Ambridge IC, Che C, Micheal H, Muir RJ, Tidwell TT. *J. Am. Chem. Soc.* 1983; **105**: 2343–2350.